Turkish Journal of Science & Technology
20(2), 495-505, 2025

Research Paper
https://doi.org/10.55525/tjst.1720588

Characteristics of AlSi10Mg Aluminum Alloy Plates Produced Through Additive Manufacturing Technique

Mehmet YAZ[1], Ömer EKİNCİ[2*], Zülküf BALALAN[3], Özgür ÖZGÜN[4]

[1] Machinery and Metal Technologies, Technical Sciences Vocational School, Firat University, Elazıg, Türkiye
[2] Astronautical Engineering, Faculty of Aeronautics and Astronautics, Sivas University of Science and Technology, Sivas, Türkiye
[3] Mechanical Engineering, Faculty of Engineering-Architecture, Bingol University, Bingol, Türkiye
[4] Occupational Health and Safety, Faculty of Health Sciences, Bingol University, Bingol, Türkiye
[1] myaz@firat.edu.tr, [2] omerekinci@sivas.edu.tr, [3] zbalalan@bingol.edu.tr, [4] oozgun@bingol.edu.tr

(Geliş/Received: 17/06/2025; Kabul/Accepted: 01/09/2025)

Abstract: The microstructure and mechanical properties of AlSi10Mg aluminum alloy sheets produced by additive manufacturing method were revealed. It was clearly observed that the microstructure consisted of weld pools separated by boundaries. Furthermore, a small number of distributed pores with diameters ranging from 35 μm to 5 μm were detected in the microstructure. A few small-sized pores are a sign of good production. Vickers microhardness of the produced AlSi10Mg alloy was measured to be average 126.625 HV. Additionally, its tensile strength and three-point bending strength value were found to be 433 MPa and 548 MPa, respectively. The tensile fracture surface had many small and deep dimples while three-point bending fracture surface also possessed dimples, however, bigger and shallower compared with that of tensile fracture. Therefore, the tensile and three-point bending tests showed a reasonable ductile fracture behavior.

Key words: Additive manufacturing, AlSi10Mg aluminum alloy, microstructure, microhardness, tensile strength, three-point bending strength.

Eklemeli İmalat Tekniğiyle Üretilen AlSi10Mg Alüminyum Alaşımlı Plakaların Özellikleri

Öz: Eklemeli imalat yöntemi ile üretilen AlSi10Mg alüminyum alaşımlı levhaların mikroyapı ve mekanik özellikleri ortaya çıkarıldı. Mikro yapının, sınırlarla ayrılmış kaynak havuzlarından oluştuğu açıkça gözlemlenmiştir. Ayrıca, mikro yapıda çapları 35 μm ile 5 μm arasında değişen az sayıda dağınık gözenek tespit edilmiştir. Birkaç küçük gözenek, iyi bir üretimin işaretidir. Üretilen AlSi10Mg alaşımının Vickers mikro sertliği ortalama 126,625 HV olarak ölçülmüştür. Ayrıca, çekme dayanımı ve üç noktalı eğilme dayanımı değerleri sırasıyla 433 MPa ve 548 MPa olarak bulunmuştur. Çekme kırılma yüzeyinde çok sayıda küçük ve derin çukur bulunurken, üç noktalı eğilme kırılma yüzeyinde de çukurlar bulunmaktaydı, ancak bu çukurlar çekme kırılmasına kıyasla daha büyük ve daha sığdı. Çekme ve üç nokta eğme testleri makul bir sünek kırılma davranışı göstermiştir.

Anahtar kelimeler: Eklemeli imalat, AlSi10Mg alüminyum alaşımı, mikroyapı, mikrosertlik, çekme dayanımı, üç nokta eğme dayanımı.

1. Giriş

Aluminum (Al) alloys are widely used in the aerospace, automotive, and transportation sectors because of their outstanding properties [1,2]. AlSi10Mg is a typical Al alloy that has grown in popularity in a variety of industries, including aerospace, transportation, and equipment production because of its characteristics, such as high strength/weight ratio, low thermal expansion coefficient, and good resistance to corrosion and wear [3-6]. AlSi10Mg is a typical traditional-cast aluminum alloy [7]. Nevertheless, the AlSi10Mg alloy produced through conventional casting has issues with coarse structure, low strength, and a mismatch between strength and plasticity, which restricts its potential for further development and use in specific service conditions [8,9]. Also, it is challenging to produce AlSi10Mg with complicated geometries to meet the requirements using traditional techniques [10,11]. Additive manufacturing (AM), also known as three-dimensional (3D) printing, can fabricate complex components for use in the aerospace, medical, and automotive sectors [12-15]. AM has been rising steadily in popularity recently since it can cope with difficulties with traditional manufacturing techniques, based on the direct fabrication of near-net form components from three-dimensional (3D) models without needing a tool [16]. AM technology gave industries previously unthinkable opportunities to make components with intricate

* Corresponding author: omerekinci@sivas.edu.tr. ORCID Number of authors: [1] 0000-0002-5422-7433, [2] 0000-0002-0179-6456, [3] 0000-0001-5808-6263, [4] 0000-0003-3816-6746

freeform geometries, which are extremely challenging or impossible to achieve using traditional manufacturing methods [17,18]. Laser powder bed fusion (LPBF), one of the AM processes, can produce three-dimensional products directly from a computer-aided design (CAD) file [19,20]. LPBF is one of the most attractive processes for creating intricate metal parts with high geometric precision among the AM methods [21]. As the weldability of AlSi10Mg is good, LPBF has gained popularity for fabricating AlSi10Mg components owing to its superior sample shaping precision and resolution and also its ability to produce finer features and smoother surface finishes [22,23]. AlSi10Mg has distinctive microstructures and mechanical characteristics due to the high cooling rate and temperature gradient during LPBF [24]. According to Kempen et al. [25], the fine microstructure of the AlSi10Mg parts produced by LPBF results in greater levels of hardness, tensile strength, and elongation when compared to their cast equivalents. According to Aktürk and Korkmaz [26], products produced using AM are more homogeneous than their casting counterparts, resulting in higher yield and rupture strengths. The key factors contributing to this homogeneity are the particle size and the mixing ratio of the powder mixture. Accurately determining the composition of the materials used in additive manufacturing is crucial, as it directly impacts the final product. According to Read et al. [27], AlSi10Mg has a noticeably longer rupture lifetime when it is made using the ideal LPBF process settings. In addition, since AlSi10Mg produced by the AM exhibits excellent mechanical properties at high temperatures, it offers a lot of promise for use in a variety of applications over a broad temperature range [28,29]. It is reported that the AlSi10Mg composite made via LPBF showed improved tensile strength at higher temperatures [30]. Kartal [31] studied the optimization of production parameters to obtain the best mechanical properties of 3D printed parts from a Polylactic Acid (PLA) and Walnut Shell Composite via the Taguchi method. It was concluded that the deposition angle was the most effective parameter. The primary benefit of 3D printers is their ability to easily and efficiently design and manufacture extremely complex structures that are impossible to produce using CNC machines. The usage of 3-D printer technology has begun to spread across several industries, including aerospace and agriculture. The engineering and scientific world in the realm of electromagnetics are also drawn to 3-D printed materials [32]. The use of additive manufacturing method is increasing day by day and determining the production parameters and mechanical properties of the produced parts is becoming increasingly important [33]. With the development of metal AM technology, direct part production has become easier, which is a significant advantage to produce metal parts used in rail systems. To build a smart railway line, AM should be adopted in the railway industry and its usage potential should be increased [34]. It's clear that AM will become an increasingly important part of our lives in the future. This technology will eliminate the need for large-scale production in facilities located in just a few locations; parts can be manufactured across a much wider geography. It's not unreasonable to imagine a future where organs will be printed in hospitals, and additive manufacturing technology systems will allow everyone to print the parts they need at home, particularly with personalized production [35].

2. Material and Method

AlSi10Mg aluminum alloy powder with a diameter ranging from 20 to 63 μm was used to produce AlSi10Mg alloy plates. The scanning electron microscope (SEM) image of the AlSi10Mg powder is shown in Figure 1. Energy Dispersive Spectrometry (EDS) elemental weight percentage analysis was carried out, and the obtained result is given in Figure 2. Accordingly, 87.51 percent Al, 11.82 Si, 0.39 Mg, and 0.27 Fe were found by weight. AlSi10Mg aluminum alloy consists mostly of Al, Si and Mg. Generally, AlSi10Mg contains 89-91% Al, 9-11% Si and 0.2-0.45% Mg. The base metal, Al, provides lightness and corrosion resistance [36]. Si provides good fluidity and castability, as well as increasing strength and hardness. Mg increases strength through solid solution strengthening and precipitation hardening. Small amounts of Fe are also present as an impurity element. Fe, tighter control over composition allows this alloy powder to achieve better consistency in final part properties [37]. Fe is kept low to maintain ductility and corrosion resistance [36]. TESCAN model MIRA 3 machine was used for SEM and EDS analysis. Ermaksan model laser powder bed fusion additive manufacturing machine was utilized for manufacturing AlSi10Mg plates as seen in Figure 3. 2 mm thick, 60 mm wide and 100 mm length AlSi10Mg alloy plates were produced by using the parameters of layer thickness = 30μm, hatch distance (offset) = 100μm, laser spot diameter = 85 μm, scanning speed (laser speed) = 800 mm·s-1and laser power = 320W. The manufacturing process of the AlSi10Mg plates by selective laser melting (SLM) method and manufactured AlSi10Mg plates are shown in Figures 4 and 5, respectively. No heat treatment was carried out after manufacturing AlSi10Mg plates. The microstructure of the AlSi10Mg aluminum alloy was attained by INVERTED MICROSCOPE SOIF Optical Instruments MDS400 after sanding with up to 2500 grit sandpaper and polishing with broadcloth diamond suspension in Figure 6. The Vickers microhardness of AlSi10Mg aluminum alloy was measured from the polished piece with a METKON DUROLINE-M brand tester under 300 grams load and 10 seconds waiting conditions. The

tensile test specimen of AlSi10Mg alloy was produced according to ASTM 8E standard as shown in Figure 7. The tensile and three-point bending tests of AlSi10Mg alloy were performed on the SHIMADZU model tester having a maximum 50 kN load using 0.5 mm·min-1 tension and compression speed at room temperature. The fracture surfaces of the tensile and three-point bending tests of AlSi10Mg alloy were examined with SEM analysis.

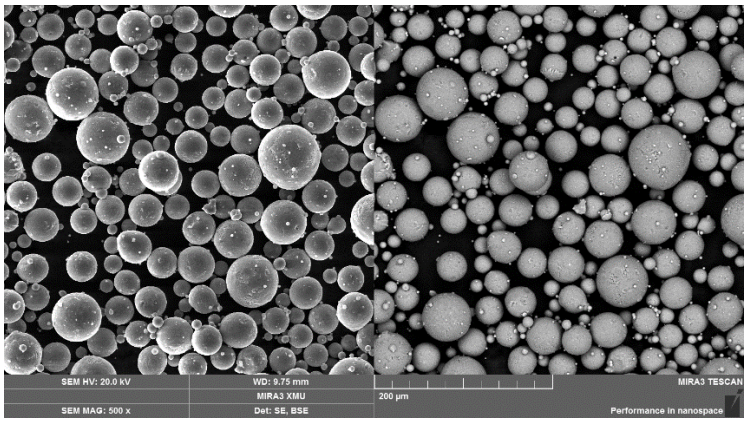

Figure 1. SEM photo of the AlSi10Mg aluminum alloy powder.

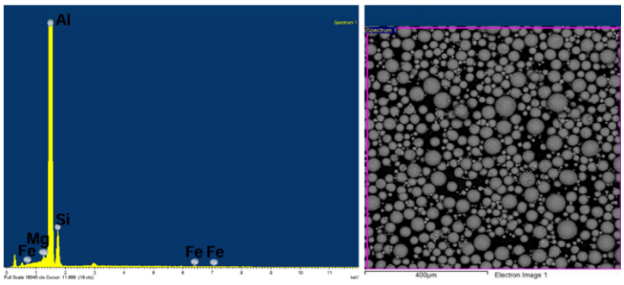

Element	Weight%
Mg	0.39
Al	87.51
Si	11.82
Fe	0.27
Totals	100

Figure 2. AlSi10Mg alloy powder EDS analysis result.

Figure 3. Laser powder bed fusion additive manufacturing machine.

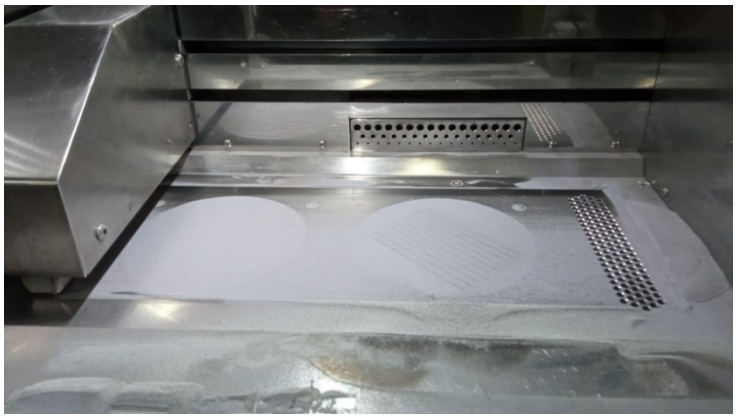

Figure 4. The manufacturing process of the AlSi10Mg aluminum alloy plates.

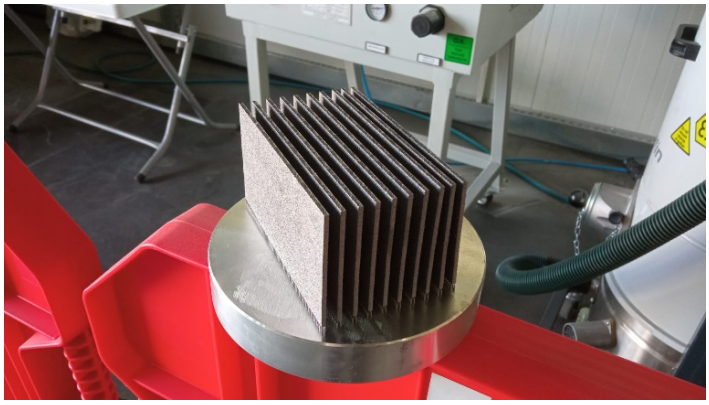

Figure 5. The manufactured AlSi10Mg aluminum alloy plates.

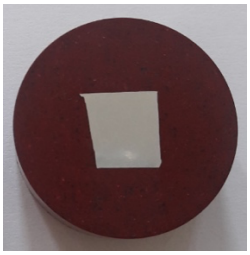

Figure 6. Sandpapered and polished piece of the AlSi10Mg aluminum alloy plate.

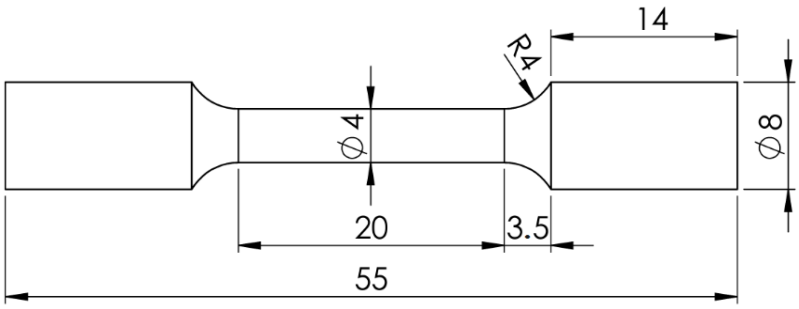

Figure 7. Tensile specimen of the AlSi10Mg alloy.

3. Results and Discussion

3.1. Microstructural analysis

As seen in Figure 1, AlSi10Mg aluminum alloy powder consists of particles with spherical and smooth surfaces. According to [38], the spherical form of the particles and their smooth surfaces would aid in achieving superior fusibility and flowability while making plates with laser melting. Figure 8 illustrates optical microscope images taken from the building direction surface of the AlSi10Mg alloy plate. Weld pools and their boundaries can be clearly seen. Very few pores were detected particularly on the weld pool boundary. Pore diameters were measured and found to vary between 35 µm and 5 µm, but only a few large pores were determined. The absence of many pores is an indication of quality manufacturing. Owing to inadequate energy density [39] and inferior overlap of melt pools (scan tracks) [40], defects, particularly pores because of lack of fusion, are present in the manufacturing of AlSi10Mg by LPBF. The pores of lack of fusion show preferred orientations in contrast to gas pores [41]. Fritsche et al. [42] also detected lack of fusion defects and pores in the AlSi10Mg produced by LPBF. According to [43], during LPBF, pores can easily develop and deteriorate the material's mechanical characteristics.

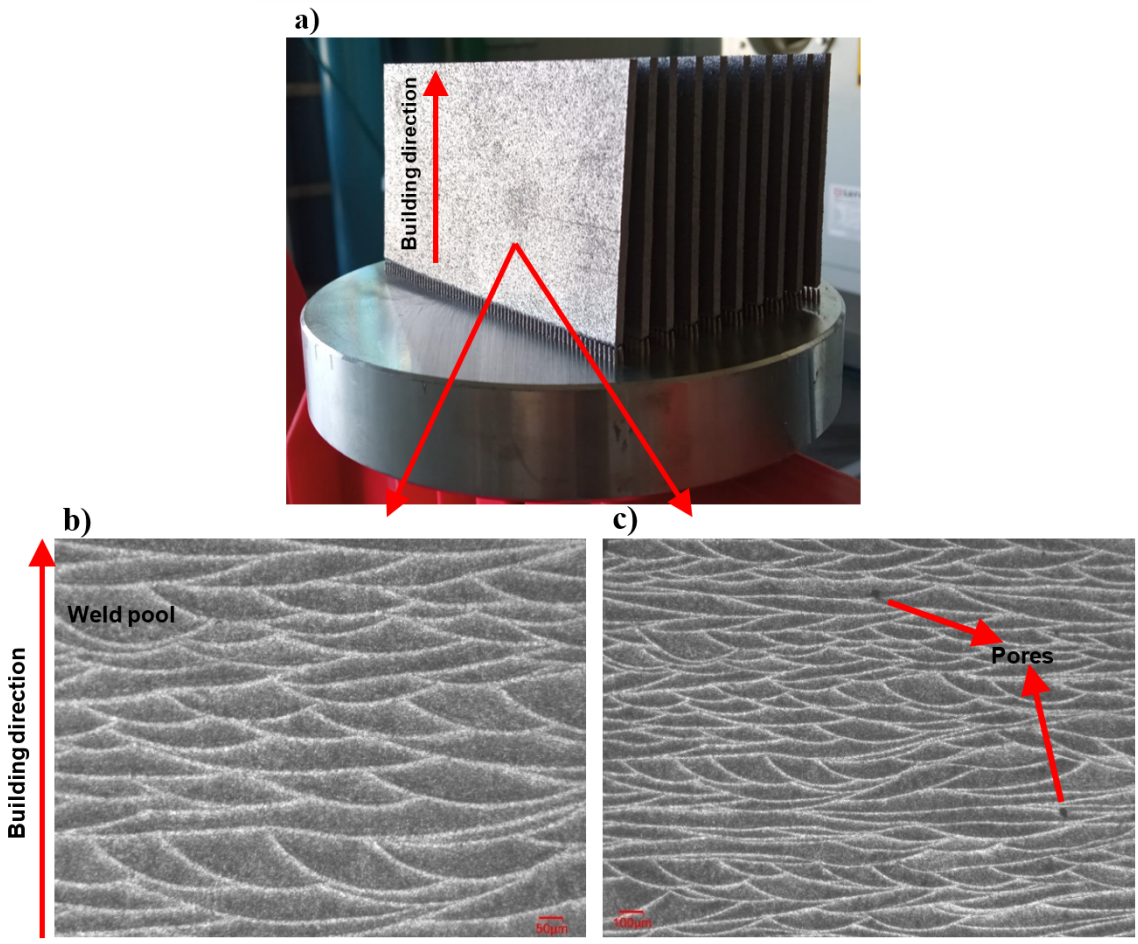

Figure 8. Microstructure of the AlSi10Mg alloy.

3.2. Microhardness analysis

Figure 9 shows the microhardness graph of AlSi10Mg alloy obtained by applying 15 microhardness measurements. The AlSi10Mg alloy was found to have an average hardness value of 126.625 HV. Kempen et. al. [25] produced AlSi10Mg alloy by the AM and determined its microhardness as 127 HV.

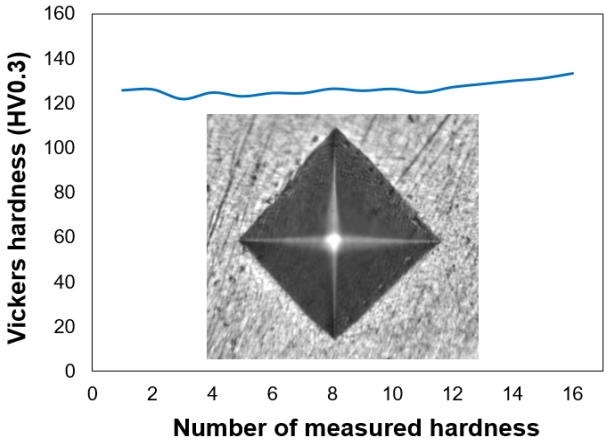

Figure 9. Microhardness of the AlSi10Mg alloy.

3.3. Tensile and three-point bending strength analysis

The tensile strength of the AlSi10Mg alloy was obtained and presented in Figure 10. AlSi10Mg alloy had a tensile strength of 433 Mpa, an elongation of 2.074 mm, and an elongation of 13.3 %. Kempen et al. [25] found the tensile strength of AlSi10Mg alloy approximately 400 Mpa. According to Kempen et al. [25], the hardness and strength of AlSi10Mg alloy manufactured by AM were higher than that of AlSi10Mg alloy produced by the traditional casting. Li et al. [44] produced AlSi10Mg alloy through the AM process and found its tensile strength as 454 Mpa. Chu et al. [45] used powder sizes 16 µm and 76 µm to produce AlSi10Mg alloy via the AM. The AlSi10Mg alloy produced with 16 µm powder had a tensile strength of 470 MPa, while 428 MPa was attained with 76 µm powder. The tensile strength value of the AlSi10Mg alloy attained in this study is consistent with other studies. According to the [46] study, the tensile strength and microhardness of the AlSi10Mg alloy manufactured via the AM are higher than that of the AlSi10Mg alloy fabricated by casting. According to Gökdağ and Acar [47], while the hardness value is proportional to the cooling rate, it is inversely proportional to the energy density.

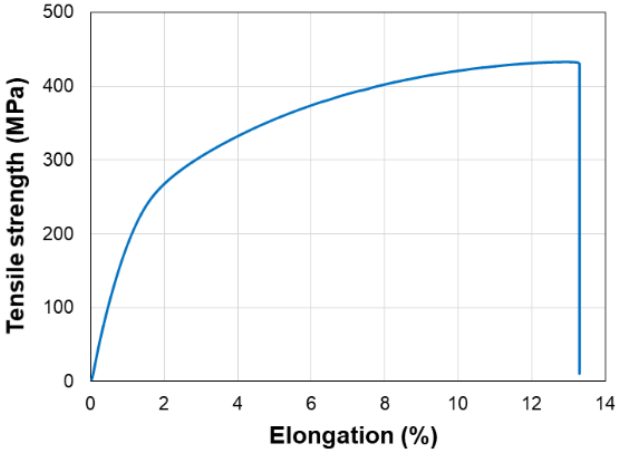

Figure 10. Tensile strength of the alsi10mg alloy.

To further assess the mechanical properties of the AlSi10Mg aluminum alloy fabricated by the AM, three-point bending test was conducted. The three-point bending strength of the AlSi10Mg aluminum alloy is in Figure 11. The support span is 28 mm, and the sample thickness, width, and length are 2.35 mm, 3.75 mm, and 45 mm, respectively. The three-point bending strength of the AlSi10Mg alloy was found to be 548 MPa.

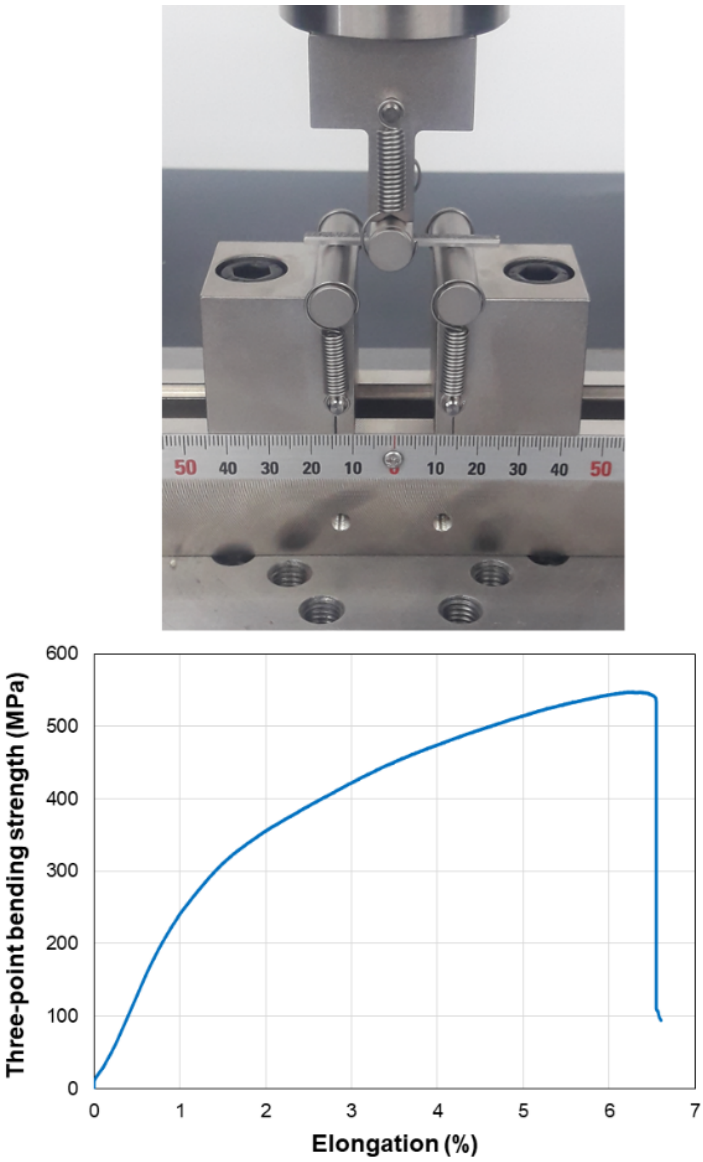

Figure 11. Three-point bending strength of the AlSi10Mg alloy.

3.4 Fracture surface

Figure 12 indicates the fractured tensile specimen of AlSi10Mg alloy in the tensile test and the SEM photograph of the fracture surface. As seen in Figure 12a, the tensile sample broke at an angle of approximately 45 degrees. Some small pores mostly circular were detected with the size of 1.5-5.5 µm in diameter at the fracture surface (Figure 12b). Since the number of pores is low and their sizes are small, it is assumed that they do not have a significant negative effect on tensile strength. Moreover, many tear ridges were observed on the fracture surface (Figure 12b). In addition, it is clear that the fracture surface consists of many fine equiaxed dimples with a size ranging between 0.39 and 0.78 µm in diameter, showing ductile fracture (Figure 12c). Consequently, the tensile fracture exhibited mainly a ductile type of plastic fracture features. Line et al. [48] also produced AlSi10Mg Alloy by SLM-type additive manufacturing and found that the tensile fracture surface was composed of numerous dimples indicating ductile mode fracture.

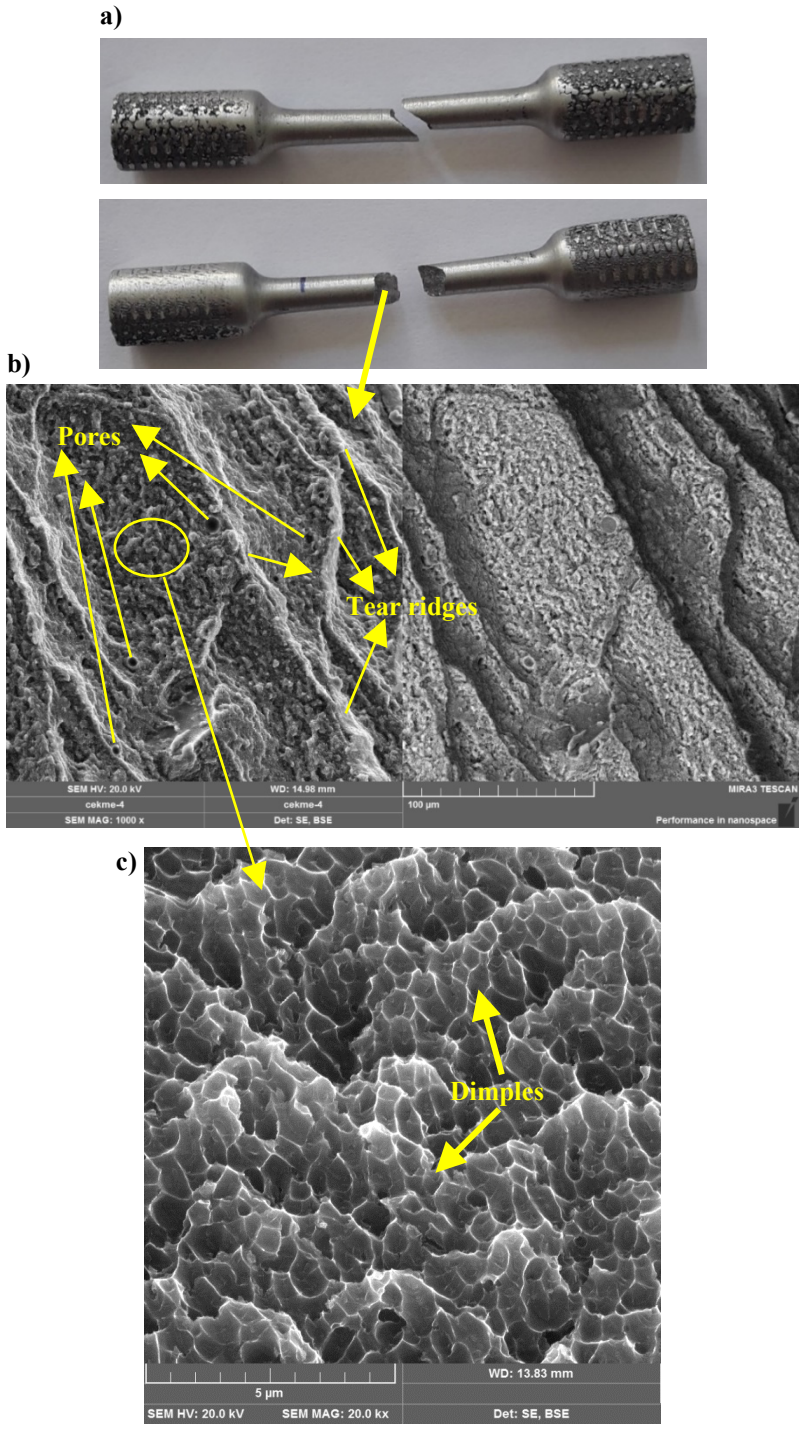

Figure 12. Tensile fracture surface.

Figure 13a and b show the photograph of the fractured three-point bending specimen and its SEM fracture surface image, respectively. As seen in Figure 13a, the three-point bending specimen broke at almost 90 degrees. It can be seen from Figure 13b that the three-point bending fracture surface consisted of many dimples, but larger and shallower compared to that of the tensile fracture in Figure 12c. This means that less ductile and less plastic fracture occurred compared to the tensile fracture. From 10 and 11, it can be seen that the elongation in percentage for tensile tests is about 13, and for three-point bending is 7. The size of dimples is ranging between 0.47 and 1

µm in diameter. Furthermore, a few pores can be seen at the fracture surface in Figure 13b. Since there are a few pores detected at the fracture area, it can be said that pores had no significant effect on the fracture strength.

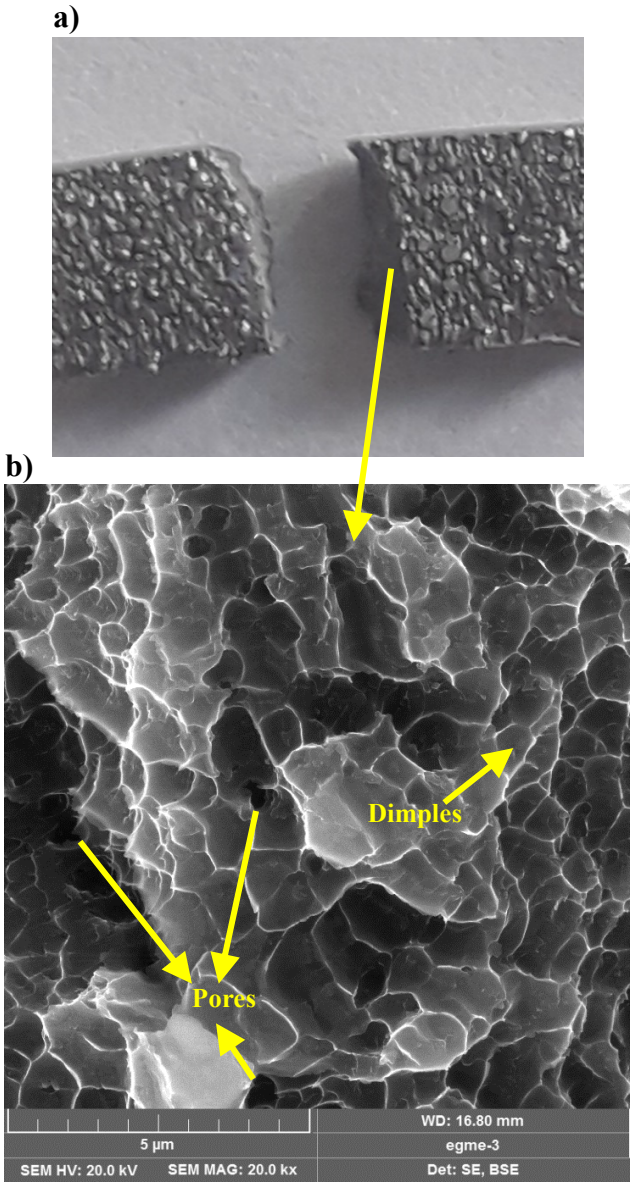

Figure 13. Three-point bending fracture surface.

4. Conclusions

AlSi10Mg aluminum alloy was successfully produced by Selective laser melting of laser powder bed fusion of additive manufacturing. The microstructure and mechanical properties of the produced AlSi10Mg were revealed and presented below.

1. AlSi10Mg alloy was fabricated with very little porosity, meaning that the production parameters used were successful.

2. The average hardness value of the produced AlSi10Mg alloy was determined to be 126.625 HV, tensile strength as 433 Mpa and three-point bending strength as 548 MPa.

3. The tensile fracture surface of the produced AlSi10Mg alloy consisted of many small dimples indicating ductile plastic fracture.

4. The three-point bending fracture surface was also comprised of dimples, but larger and shallower compared to the tensile fracture surface, indicating less ductile and plastic fracture.

5. In this study, some pores were detected in the microstructure of additively manufactured AlSi10Mg alloy parts, therefore, studies can be conducted on optimizing the production parameters or developing new methods to minimize this porosity defect and improve mechanical properties.

6. As a result of this study, it can be said that it is possible to produce AlSi10Mg alloy parts effectively using the additive manufacturing method. Since the AlSi10Mg alloy exhibits good strength and weight reduction properties, more efficient, complex-shaped housings, load-bearing and non-load-bearing structural components, etc. can be produced from the AlSi10Mg alloy for air and land vehicles by the additive manufacturing method.

Acknowledgments

This study was supported by Sivas University of Science and Technology, Scientific Research Projects Coordination Unit with Project number of 2023-GENL-Hav-0011. Ö.E. idea owner, conducted experiments and wrote the article, M.Y. conducted experiments and wrote the article, Z.B. and Ö.Ö. evaluated the results.

References

[1] You X, Xing Z, Jiang S, Zhu Y, Lin Y, Qiu H, Nie R, Yang J, Hui D, Chen W, Chen Y. A review of research on aluminum alloy materials in structural engineering. Dev Built Environ 2024; 17: 100319.
[2] Hongfu Y, Rensong H, Yelin Z, Shanju Z, Mengnie L, Koppala S, Kemacheevakul P, Sannapaneni J. Effect of rolling deformation and passes on microstructure and mechanical properties of 7075 aluminum alloy. Ceram Int 2023; 49(1): 1165-1177.
[3] Ye F, Mao L, Rong J, Zhang B, Wei L, Wen S, Jiao H, Wu S. Influence of different rolling processes on microstructure and strength of the Al-Cu-Li alloy AA2195. Prog Nat Sci-Mater 2022; 32(1): 87-95.
[4] Chen Y, Wang L, Feng Z, Zhang W. Effects of heat treatment on microstructure and mechanical properties of SLMed Sc-modified AlSi10Mg alloy. Prog Nat Sci-Mater 2021; 31(5): 714-721.
[5] Vidyasagar CHS, Karunakar D.B. Effect of spark plasma sintering and reinforcements on the formation of ultra-fine and nanograins in AA2024-TiB2-Y hybrid composites. Prog Nat Sci-Mater 2022; 32(1): 79-86.
[6] Wen K, Li X, Xiong B, Lin H, Wen Q, Li Y, Yan H, Yan L, Zhang Y, Li Z, Liu H. Near-microscopic grain boundary facilitates fatigue crack propagation in a polycrystalline Al-Zn-Mg-Cu alloy. Prog Nat Sci-Mater 2023; 33(1): 120-125.
[7] Kim DK, Hwang JH, Kim EY, Heo YU, Woo W, Choi S.H. Evaluation of the stress-strain relationship of constituent phases in AlSi10Mg alloy produced by selective laser melting using crystal plasticity FEM. J Alloy Compd 2017; 714: 687-697.
[8] Wang Z, Zhuo L, Yin E, Zhao Z. Microstructure evolution and properties of nanoparticulate SiC modified AlSi10Mg alloys. Mat Sci Eng A 2021; 808: 140864.
[9] Xue G, Ke L, Zhu H, Liao H, Zhu J, Zeng X. Influence of processing parameters on selectie laser melted SiC/AlSi10Mg composites: densification, microstructure and mechanical properties. Mat Sci Eng A 2019; 764: 138155.
[10] Li Z, Li Z, Tan Z, Xiong DB, Guo Q. Stress relaxation and the cellular structure-dependence of plastic deformation in additively manufactured AlSi10Mg alloys. Int J Plasticity 2020; 127: 102640.
[11] Tradowsky U, White J, Ward RM, Read N, Reimers W, Attallah MM. Selective laser melting of AlSi10Mg: Influence of post-processing on the microstructural and tensile properties development. Mater Design 2016; 105: 212-222.
[12] Sames WJ, List FA, Pannala S, Dehoff RR, Babu S.S. The metallurgy and processing science of metal additive manufacturing. Int Mater Rev 2016; 61(5): 315-360.
[13] Frazier WE. Metal additive manufacturing: a review. J Mater Eng Perform 2014; 23: 1917-1928.
[14] Bikas H, Stavropoulos P, Chryssolouris G. Additive manufacturing methods and modelling approaches: a critical review. Int J Adv Manuf Tech 2016; 83: 389-405.
[15] Lewandowski JJ, Seifi M. Metal additive manufacturing: a review of mechanical properties. Annu Rev Mater Res 2016; 46: 151-186.
[16] Chen B, Moon SK, Yao X, Bi G, Shen J, Umeda J, Kondoh K. Strength and strain hardening of a selective laser melted AlSi10Mg alloy. Scripta Mater 2017; 141: 45-49.
[17] Yap CY, Chua CK, Dong ZL, Liu ZH, Zhang DQ, Loh LE, Sing S.L. Review of selective laser melting: materials and applications. Appl Phys Rev 2015; 2(4): 041101.

[18] Zhang J, Song B, Wei Q, Bourell D, Shi Y. A review of selective laser melting of aluminum alloys: processing, microstructure, property and developing trends. J Mater Sci Technol 2019; 35(2): 270-284.
[19] Santos EC, Shiomi M, Osakada K, Laoui T. Rapid manufacturing of metal components by laser forming. Int J Mach Tools Manuf 2006; 46(12-13): 1459-1468.
[20] Rombouts M, Kruth JP, Froyen L, Mercelis P. Fundamentals of selective laser melting of alloyed steel powders. Cirp Ann-Manuf Techn 2006; 55(1): 187-192.
[21] Du Z, Tan MJ, Chen H, Bi G, Chua CK. Joining of 3D-printed AlSi10Mg by friction stir welding. Weld World 2018; 62(3): 675-682.
[22] Herzog D, Seyda V, Wycisk E, Emmelmann C. Additive manufacturing of metals. Acta Mater 2016; 117: 371-392.
[23] DebRoy T, Wei HL, Zuback JS, Mukherjee T, Elmer JW, Milewski JO, Beese AM, Wilson-Heid A, De A, Zhang W. Additive manufacturing of metallic components-Process, structure and properties. Prog Mater Sci 2018; 92: 112-224.
[24] Dai S, Hu D, Grilli N, Zou S, Deng Z, Yan W. Anisotropic and high-temperature deformation behavior of additively manufactured AlSi10Mg: experiments and microscale modeling. Addit Manuf 2024; 89: 104285.
[25] Kempen K, Thijs L, Van Humbeeck J, Kruth JP. Mechanical properties of AlSi10Mg produced by selective laser melting. Phys Procedia 2012; 39: 439-446.
[26] Aktürk M, Korkmaz ME. A review on determination of material constitutive parameters of aluminum alloys produced by additive manufacturing method. MATECA 2021; 2(1): 49-60.
[27] Read N, Wang W, Essa K, Attallah MM. Selective laser melting of AlSi10Mg alloy: Process optimisation and mechanical properties development. Mater Design (1980-2015) 2015; 65: 417-424.
[28] Alhammadi A, Al-Ketan O, Khan KA, Ali M, Rowshan R, Abu Al-Rub RK. Microstructural characterization and thermomechanical behavior of additively manufactured AlSi10Mg sheet cellular materials. Mat Sci Eng A 2020; 791: 139714.
[29] Uzan NE, Shneck R, Yeheskel O, Frage N. High-temperature mechanical properties of AlSi10Mg specimens fabricated by additive manufacturing using selective laser melting technologies (AM-SLM). Addit Manuf 2018; 24: 257-263.
[30] He P, Kong H, Liu Q, Ferry M, Kruzic JJ, Li X. Elevated temperature mechanical properties of TiCN reinforced AlSi10Mg fabricated by laser powder bed fusion additive manufacturing. Mat Sci Eng A 2021; 811: 141025.
[31] Kartal F. Mechanical performance optimization in FFF 3D printing using Taguchi design and machine learning approach with PLA/walnut Shell composites filaments. J. Vinyl Addit. Technol. 2025; 31: 622-638.
[32] Bakır M. 3-D Printed Dual-Band Frequency Selective Surfaces for Radome Applications. TJST 2023; 18(1): 169-176.
[33] Akçay Ö, Arı A. Effect of infill density and infill pattern on mechanical properties of 3D-printed PLA produced by FFF. FÜMBD 2025; 37(1); 223-232.
[34] Aslan İ, Can A. A review on the use of additive manufacturing technology in the railway industry. KSU J Eng Sci 2023; 26(4): 1078-1096.
[35] Özer G. A review on additive manufacturing technologies. NOHU J Eng Sci 2020; 9(1): 606-621.
[36] https://aludiecasting.com/tr/alsi10mg-dokum/ Access Date: 21.07.2025.
[37] https://met3dp.com/tr/aluminum-alsi10mg-powder-a-technical-overview/ Access Date: 21.07.2025.
[38] Yan C, Hao L, Hussein A, Bubb SL, Young P, Raymont D. Evaluation of light weight AlSi10Mg periodic cellular lattice structures fabricated via direct metal laser sintering. J Mater Process Techn 2014; 214(4): 856-864.
[39] Yang KV, Rometsch P, Jarvis T, Rao J, Cao S, Davies C, Wu X. Porosity formation mechanisms and fatigue response in Al-Si-Mg alloys made by selective laser melting. Mat Sci Eng A 2018; 712: 166-174.
[40] Tang M, Pistorius PC, Beuth JL. Prediction of lack-of-fusion porosity for powder bed fusion. Addit Manuf 2017; 14: 39-48.
[41] Wu Z, Wu S, Bao J, Qian W, Karabal S, Sun W, Withers PJ. The effect of defect population on the anisotropic fatigue resistance of AlSi10Mg alloy fabricated by laser powder bed fusion. Int J Fatigue 2021; 151: 106317.
[42] Fritsche S, Draper J, Toumpis A, Galloway A, Amancio-Filho ST. Refill friction stir spot welding of AlSi10Mg alloy produced by laser powder bed fusion to wrought AA7075-T6 alloy. Manuf Lett 2022; 34: 78-81.
[43] Wang Z, Xiao Z, Tse Y, Huang C, Zhang W. Optimization of processing parameters and establishment of a relationship between microstructure and mechanical properties of SLM titanium alloy. Opt Laser Technol 2019; 112: 159-167.
[44] Li C, Zhang WX, Yang HO, Wan J, Huang XX, Chen YZ. Microstructural origin of high strength and high strain hardening capability of a laser powder bed fused AlSi10Mg alloy. J Mater Res Technol 2024; 197: 194-206.
[45] Chu F, Shen H, Liu J, Hou J, Zhang K, Zhou Z, Zhu Y, Wu X, Huang A. Improved ductility by reducing powder size in laser powder bed fusion of AlSi10Mg. Addit Manuf Front 2024; 3: 200122.
[46] Atar B, Üyüklü E, Yayla P. Microstructure and mechanical properties of an additively manufactured AlSi10Mg based alloy. Mater Test 2023; 65(6): 874-885.
[47] Gökdağ İ, Acar E. Effects of process parameters on strengthening mechanisms of additively manufactured AlSi10Mg. Mater Test 2023; 65(3): 409-422.
[48] Li Y, Gu D, Zhang H, Xi L. Effect of trace addition of ceramic on microstructure development and mechanical properties of selective laser melted AlSi10Mg alloy. Chin J Mech Eng 2020; 33: 33.